El cuadro contenía un archivo PDF; haga clic aquí para verlo

Single-shot digital holography by use of the fractional Talbot effect

Lluís Martínez-León[1], María Araiza-E[2], Bahram Javidi[3], Pedro Andrés[4], Vicent Climent[1], Jesús Lancis[1], and Enrique Tajahuerce[1*]

[1] *GROC·UJI, Departament de Física, Universitat Jaume I, 12071 Castelló, Spain.*
[2] *PDS, Unidad Académica de Ingeniería Eléctrica, Universidad Autónoma de Zacatecas, Zacatecas, México.*
[3] *Department of Electrical and Systems Engineering, University of Connecticut, CT 06269-2157 Storrs, USA.*
[4] *Departamento de Óptica, Universitat de València, 46100 Burjassot, Spain.*
**enrique.tajahuerce@uji.es*

Abstract: We present a method for recording in-line single-shot digital holograms based on the fractional Talbot effect. In our system, an image sensor records the interference between the light field scattered by the object and a properly codified parallel reference beam. A simple binary two-dimensional periodic grating is used to codify the reference beam generating a periodic three-step phase distribution over the sensor plane by fractional Talbot effect. This provides a method to perform single-shot phase-shifting interferometry at frame rates only limited by the sensor capabilities. Our technique is well adapted for dynamic wavefront sensing applications. Images of the object are digitally reconstructed from the digital hologram. Both computer simulations and experimental results are presented.

OCIS codes: (090.0090) Holography; (090.1760) Computer holography; (100.6890) Three-dimensional image processing; (100.3010) Image reconstruction techniques; (070.6760) Talbot effect; (120.3180) Interferometry; (050.5080) Phase shift.

References and links

1. U. Schnars, and W. P. O. Jüptner, "Digital recording and numerical reconstruction of holograms," Meas. Sci. Technol. **13**(9), 85–101 (2002).
2. J. W. Goodman, and R. W. Lawrence, "Digital image formation from electronically detected holograms," Appl. Phys. Lett. **11**(3), 77–79 (1967).
3. M. A. Kronrod, N. S. Merzlyakov, and L. P. Yaroslavsky, "Reconstruction of holograms with a computer," Sov. Phys. Tech. Phys. **17**, 333–334 (1972).
4. L. Onural, and P. D. Scott, "Digital decoding of in-line holograms," Opt. Eng. **26**, 1124–1132 (1987).
5. U. Schnars, and W. P. O. Jüptner, "Direct recording of holograms by a CCD target and numerical reconstruction," Appl. Opt. **33**(2), 179–181 (1994).
6. I. Yamaguchi, and T. Zhang, "Phase-shifting digital holography," Opt. Lett. **22**(16), 1268–1270 (1997).
7. E. Cuche, F. Bevilacqua, and C. Depeursinge, "Digital holography for quantitative phase-contrast imaging," Opt. Lett. **24**(5), 291–293 (1999).
8. F. Dubois, L. Joannes, and J.-C. Legros, "Improved three-dimensional imaging with a digital holography microscope with a source of partial spatial coherence," Appl. Opt. **38**(34), 7085–7094 (1999).
9. G. Pedrini, and H. J. Tiziani, "Short-coherence digital microscopy by use of a lensless holographic imaging system," Appl. Opt. **41**(22), 4489–4496 (2002).
10. L. Martínez-León, G. Pedrini, and W. Osten, "Applications of short-coherence digital holography in microscopy," Appl. Opt. **44**(19), 3977–3984 (2005).
11. Y. Frauel, T. Naughton, O. Matoba, E. Tajahuerce, and B. Javidi, "Three Dimensional Imaging and Display Using Computational Holographic Imaging," Proc. IEEE **94**(3), 636–654 (2006).
12. B. Javidi, S. Yeom, and I. Moon, "Real-time 3D sensing, visualization and recognition of biological microorganisms," Proc. IEEE **94**(3), 550–567 (2006).
13. B. Javidi, and T. Nomura, "Securing information by use of digital holography," Opt. Lett. **25**(1), 28–30 (2000).
14. E. Tajahuerce, and B. Javidi, "Encrypting three-dimensional information with digital holography," Appl. Opt. **39**(35), 6595–6601 (2000).
15. O. Matoba, and B. Javidi, "Optical retrieval of encrypted digital holograms for secure real-time display," Opt. Lett. **27**(5), 321–323 (2002).
16. B. Javidi, and E. Tajahuerce, "Three-dimensional object recognition by use of digital holography," Opt. Lett. **25**(9), 610–612 (2000).
17. E. Tajahuerce, O. Matoba, and B. Javidi, "Shift-invariant three-dimensional object recognition by means of digital holography," Appl. Opt. **40**(23), 3877–3886 (2001).

#111787 - $15.00 USD Received 22 May 2009; revised 26 Jun 2009; accepted 28 Jun 2009; published 13 Jul 2009

18. Y. Frauel, E. Tajahuerce, M.-A. Castro, and B. Javidi, "Distortion-tolerant 3D object recognition using digital holography," Appl. Opt. **40**, 3887–3893 (2001).
19. L. Xu, X. Peng, Z. Guo, J. Miao, and A. Asundi, "Imaging analysis of digital holography," Opt. Express **13**(7), 2444–2452 (2005).
20. X. F. Meng, L. Z. Cai, X. F. Xu, X. L. Yang, X. X. Shen, G. Y. Dong, and Y. R. Wang, "Two-step phase-shifting interferometry and its application in image encryption," Opt. Lett. **31**(10), 1414–1416 (2006).
21. A. Hettwer, J. Kranz, and J. Schwider, "Three channel phase-shifting interferometer using polarization-optics and a diffraction grating," Opt. Eng. **39**(4), 960–966 (2000).
22. J. Millerd, N. Brock, J. Hayes, M. North-Morris, M. Novak, and J. C. Wyant, "Pixelated phase-mask dynamic interferometer," Proc. SPIE **5531**, 304–314 (2004).
23. M. Novak, J. Millerd, N. Brock, M. North-Morris, J. Hayes, and J. Wyant, "Analysis of a micropolarizer array-based simultaneous phase-shifting interferometer," Appl. Opt. **44**(32), 6861–6868 (2005).
24. Y. Awatsuji, M. Sasada, and T. Kubota, "Parallel quasi-phase shifting digital holography," Appl. Phys. Lett. **85**(6), 1069–1071 (2004).
25. Y. Awatsuji, A. Fujii, T. Kubota, and O. Matoba, "Parallel three-step phase-shifting digital holography," Appl. Opt. **45**(13), 2995–3002 (2006).
26. Y. Awatsuji, T. Tahara, A. Kaneko, T. Koyama, K. Nishio, S. Ura, T. Kubota, and O. Matoba, "Parallel two-step phase-shifting digital holography," Appl. Opt. **47**(19), 183–189 (2008).
27. T. Nomura, S. Murata, E. Nitanai, and T. Numata, "Phase-shifting digital holography with a phase difference between orthogonal polarizations," Appl. Opt. **45**(20), 4873–4877 (2006).
28. T. M. Kreis, and W. P. O. Jüptner, "Suppression of the dc term in digital holography," Opt. Eng. **37**(8), 2357–2360 (1997).
29. B. Javidi, and D. Kim, "Three-dimensional-object recognition by use of single-exposure on-axis digital holography," Opt. Lett. **30**(3), 236–238 (2005).
30. J. T. Winthrop, and C. R. Worthington, "Theory of Fresnel images: I," J. Opt. Soc. Am. **55**(4), 373–381 (1965).
31. J. R. Leger, and G. J. Swanson, "Efficient array illuminator using binary-optics phase plates at fractional Talbot planes," Opt. Lett. **15**(5), 288–290 (1990).
32. A. W. Lohmann, and J. A. Thomas, "Making an array illuminator based on the Talbot effect," Appl. Opt. **29**(29), 4337–4340 (1990).
33. V. Arrizón, and J. Ojeda-Castañeda, "Multilevel phase gratings for array illuminators," Appl. Opt. **33**(25), 5925–5931 (1994).
34. J. Werterholm, J. Turunen, and J. Huttunen, "Fresnel diffraction in fractional Talbot planes: a new formulation," J. Opt. Soc. Am. A **11**(4), 1283–1290 (1994).
35. C. Zhou, and L. Liu, "Simple equations for the calculation of a multilevel phase grating for Talbot array illumination," Opt. Commun. **115**(1-2), 40–44 (1995).
36. A. Kolodziejczyk, Z. Jaroszewicz, A. Kowalik, and O. Quintero, "Kinoform sampling filter," Opt. Commun. **200**(1-6), 35–42 (2001).
37. A. Lohmann, and D. E. Silva, "An interferometer based on the Talbot effect," Opt. Commun. **2**(9), 413–415 (1971).
38. N. H. Salama, D. Patrignani, L. De Pasquale, and E. E. Sicre, "Wavefront sensor using the Talbot effect," Opt. Laser Technol. **31**(4), 269–272 (1999).
39. S. De Nicola, P. Ferraro, G. Coppola, A. Finizio, G. Pierattini, and S. Grilli, "Talbot self-image effect in digital holography and its application to spectrometry," Opt. Lett. **29**(1), 104–106 (2004).
40. A. Fajst, M. Sypek, M. Makowski, J. Suszek, and A. Kolodziejczyk, "Self-imaging phase mask used in digital holography with phase-shifting," Proc. SPIE **7141**, 1–7 (2008).
41. V. Arrizón, G. Rojo-Velázquez; Victor Arrizón and Gustavo Rojo-Velázquez, "Fractional Talbot field of finite gratings: compact analytical formulation," J. Opt. Soc. Am. A **18**(6), 1252–1255 (2001).

1. Introduction

Digital holography has proved to be a useful technique to measure the complex amplitude distribution associated to diffracted light beams [1]. It derived from conventional holography but involves digital sampling and numerical processing of interference patterns [2,3]. Its success was made possible in part by taking advantage of the great progress in the fabrication of CCD and CMOS image sensors [4–6]. Among many others, current applications include three-dimensional (3D) imaging and microscopy [4–12], optical encryption [13-15], and pattern recognition [16–18].

In digital holography an image sensor records the interference pattern between the light beam scattered by the object under study and a reference beam. This interference pattern is processed in the computer to reconstruct an image of the diffracting object by simulating the reference and using a Fresnel propagation algorithm. The first and more direct approach to avoid spatial overlapping between holographic twin images and zero order is to use off-axis geometries to record the digital hologram [5,7,13]. However, the pixel size of actual digital cameras and the requirement to separate the different orders in the reconstruction window

#111787 - $15.00 USD Received 22 May 2009; revised 26 Jun 2009; accepted 28 Jun 2009; published 13 Jul 2009

with the proper carrier spatial frequency limit the maximum spatial frequency of the interference pattern and the size of the object to be reconstructed. Actually, it has been shown that the space-bandwidth product of in-line digital holographic systems is better in a factor of 4 than that of off-axis configurations thus allowing for a larger effective field of view and a higher imaging resolution [19]. Therefore, phase-shifting in-line digital holography is an interesting alternative to exploit efficiently the limited spatial resolution of current digital sensors [6,9,14]. In this technique, several interferograms are recorded, each with a phase-shifted version of the reference beam, and combined to obtain just the object wavefront. Four different interference patterns are usually combined although it has been proved that it is possible to get good results with just two [20]. Nevertheless, phase-shifting in-line methods imply more complex optical systems than off-axis techniques and require sequential acquisition. Therefore they are not well adapted to measure dynamic wavefronts.

To allow time-resolved measurement, several single-shot phase-shifting techniques have been introduced [21–27]. The point is the simultaneous acquisition of several interferograms at the expense of a loss in the spatial resolution. In one approach, specific diffractive optical elements are designed to separate the different interferograms in different spatial regions of the image sensor [25]. Phase-shifting is performed through polarizing elements. This method has allowed developing dynamic wavefront analyzers. Another approach takes advantage of the periodic nature of sensor arrays [26–31]. In this case, spatial division-multiplexing is applied periodically and each phase-shifted interferogram is acquired by sampling the sensor array. However, the method requires using pixelated polarizer devices, such as retarder wave plates or linear polarizers, which are difficult to fabricate and hard to integrate with the CCD sensor, and may require relay optical systems introducing undesirable aberrations. Nevertheless, these methods have been used with success to record digital holograms using three and even two phase shifting steps [24–27]. Finally, other techniques have been proposed that are able to deal with vibrations and to work with moving objects based on computational post-processing [28] or for specific applications such as pattern recognition [29].

In this paper we present a new method for recording single-shot digital holograms based on the fractional Talbot effect. The Talbot effect or self-imaging phenomenon is observed when a grating is illuminated by a coherent light beam [30]. Under parallel illumination, replicas of the grating appear periodically at distances multiple of the Talbot distance. A superposition of shifted replicas of the grating but weighted by different phase factors, referred as Fresnel images, appear at fractions of the Talbot distance [30–36]. This property has been extensively used to develop efficient Talbot array illuminators or kinoform sampling filters [31–36]. The Talbot effect has been applied also to shearing interferometers for wavefront sensing [37,38]. Digital holography has been used to analyze the Talbot effect and its application to spectrometry [39]. In the course of submitting the manuscript we were made aware of a recent approach to perform parallel phase-shifting digital holography by using the self-imaging effect of a periodic phase mask located at the reference beam [40].

In our Talbot-based dynamic digital holography system, a conventional two-dimensional (2D) binary amplitude grating is used to codify the reference beam in an interferometer. This grating generates a periodic three-step phase distribution with uniform irradiance over the sensor plane by fractional Talbot effect. The sensor records only one interferogram between the Talbot codified reference beam and the light field scattered by the object. Different pixels of the sensor record the interferogram with different phase shifts, and the hologram is obtained by sampling and processing the pixelated phase-shifted interferogram. Therefore, our method is able to characterize dynamic wavefronts with a time resolution only limited by the acquisition time of the sensor. Compared with off-axis techniques, our optical setup is also very simple and compact but it does not require a tilted reference beam and allows an easy suppression of the zero and twin image terms. In contrast with other phase-shifting techniques, our system does not require special diffractive elements or complex pixelated polarization devices and, because of the reference amplitude modulation, it is easily adjustable to different wavelengths. Once the digital hologram has been generated, images of the object are digitally reconstructed. Both computer simulations and experimental results are presented.

#111787 - $15.00 USD Received 22 May 2009; revised 26 Jun 2009; accepted 28 Jun 2009; published 13 Jul 2009

In Section 2 we describe the basic principle of the method to perform single-shot digital holography. In Section 3 we report some computer simulations while experimental results are presented in Section 4. Finally, in Section 5 we discuss conclusions and future applications.

2. Basic layout of the system for Talbot digital holography

Our Talbot digital holographic system is based on a Mach-Zehnder interferometer with a 2D binary amplitude grating codifying the reference beam, as is shown in Fig. 1. In this optical setup, a laser beam is spatial filtered, collimated and divided by a beam splitter into an object path and a reference path in order to obtain two uniform plane waves travelling in different directions. After reflecting in a mirror, the object beam illuminates the input object, and the light scattered travels towards the CCD detector through a second beam splitter. The complex amplitude distribution, $O(x,y,z)$, of the light field diffracted by the object at a location (x,y,z) is the superposition of the spherical waves emitted by different points of the input object. Let us write the complex amplitude in the plane of the CCD, located at $z = 0$, in the following form:

$$O(x,y,0) = A_O(x,y)e^{i\phi_O(x,y)}, \tag{1}$$

where $A_O(x,y)$ and $\varphi_O(x,y)$ denote the amplitude and phase of the diffracted light field. Our objective is to measure both parameters to be able to reconstruct the complex amplitude distribution $O(x,y,z)$ at different distances z.

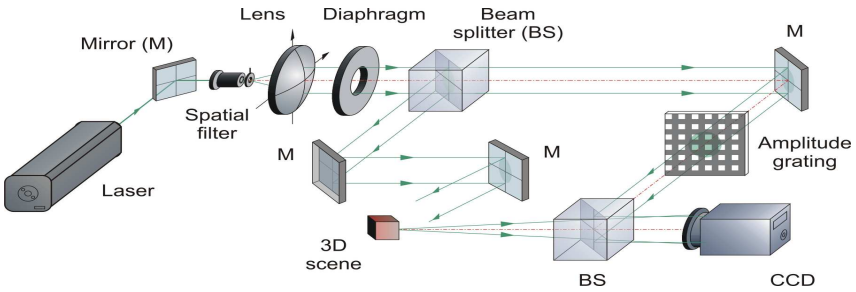

Fig. 1. Optical system for recording digital holograms by fractional Talbot effect.

The parallel reference beam, after being reflected by a mirror, is diffracted by a 2D binary amplitude grating (see Fig. 1). The diffracted light beam travels towards the sensor after reflecting in the second beam splitter. The system is aligned in such a way that the reference beam generates a plane wave traveling perpendicular to the sensor when the 2D grating is absent. The amplitude transmittance $t(x,y)$ of the grating can be written as follows:

$$t(x,y) = t_c(x,y) \otimes \left[\sum_{j=-P/2}^{P/2-1} \sum_{k=-P/2}^{P/2-1} \delta(x - j\,d)\ \delta(y - k\,d) \right], \tag{2}$$

where $t_c(x,y)$ is the amplitude transmittance of the unit cell, $\otimes$ denotes convolution, d is the period of the array, P is the number of periods, $\delta(x)$ represents the Dirac delta function, and j and k are integer numbers.

Since $t(x,y)$ is a periodic function, the amplitude distribution associated with the grating produces self-images by free-space propagation, i.e., diffraction patterns that are a copy of the input distribution, but also Fresnel images, as is shown in Fig. 2. In each transversal dimension, the former diffraction patterns consist of the superposition of r phase-weighted copies of the input grating shifted by integer multiples of d/r. Under monochromatic illumination, the Fresnel images are obtained at distances [30]

$$z' = \frac{2d^2}{\lambda}\left(q + \frac{n}{m}\right) = z_t\left(q + \frac{n}{m}\right), \tag{3}$$

#111787 - $15.00 USD Received 22 May 2009; revised 26 Jun 2009; accepted 28 Jun 2009; published 13 Jul 2009

where z_t is the so-called Talbot distance, q is an integer, and n and m are natural numbers with no common factor (with $n<m$). The ratio n/m determines the amplitude distribution at the unit cell of a particular Fresnel image. Different values of q lead simply to different positions of the Fresnel image. The number of replicas, r, associated with the Fresnel image of index n/m is given by $m/2$ when m is even and by m when m is odd. By choosing the opening ratio of the grating in accordance with the index n/m of the Fresnel image it is possible to get a uniform irradiance distribution with a periodic multilevel phase at the output plane.

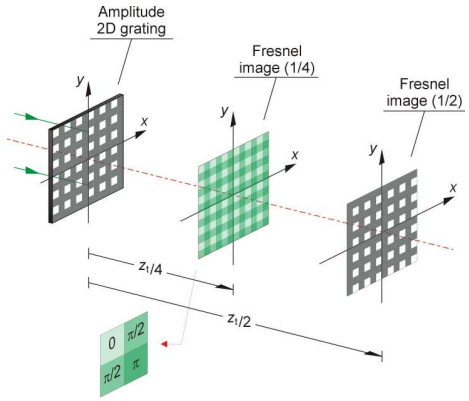

Fig. 2. Schematic diagram of the phase distribution at the 1/4 fractional Talbot plane provided by an amplitude 2D grating, and the corresponding irradiance distribution at the 1/2 Talbot plane. The magnified unit cell shows the different phases obtained at the 1/4 Fresnel image.

Several formulations have been proposed to evaluate the weighting phase factors of Fresnel images [30–36]. As we are interested in just three different phases at the output plane we restrict our analysis to the particular case n/m = 1/4 or 3/4. However other orders of the Fresnel image can be interesting to obtain more complex periodic phase distributions. For our case, the amplitude distribution generated by the reference beam at the output plane, at a distance given by Eq. (3), with n/m = 1/4 and q arbitrary, is:

$$R(x,y,0)=\frac{\mathrm{A}}{2}\left[t(x,y)+it\left(x+\frac{d}{2},y\right)+it\left(x,y+\frac{d}{2}\right)+i^2t\left(x+\frac{d}{2},y+\frac{d}{2}\right)\right], \quad (4)$$

where A is the constant amplitude of the reference beam just before the grating, assumed equal to unity in the analysis that follows. To get a Fresnel image with uniform irradiance, the amplitude transmittance, $t_c(x,y)$, of the unit cell of the grating in Eq. (2) should be given by

$$t_c(x,y)=rect\left(\frac{x}{d/2}\right)rect\left(\frac{y}{d/2}\right). \quad (5)$$

Therefore, we are able to obtain three different phase factors, 0, π/2 and π at the unit cell, distributed as is shown in Fig. 2, with uniform irradiance.

For practical purposes, it is important to consider the effect of using a finite grating in Eq. (2) in order to achieve the amplitude distribution in Eq. (4). It has been shown that the number of periods P of the grating and the number of periods P' of the Fresnel image must fulfill two restrictions, the first one to guarantee the proper profile of the Fresnel image and the second imposed by the paraxial approximation [41]. In our case, we must require

$$P>>8\frac{n}{m} \quad \text{and} \quad P+P'<<4\frac{d}{\lambda}\left(q+\frac{n}{m}\right). \quad (6)$$

When the amplitude distribution generated by the object beam, $O(x,y,0)$, in Eq. (1) interferes with that of the Talbot-codified reference beam $R(x,y,0)$ in Eq. (4) we obtain a pixelated interferogram with different periodic phase shifts. Two approaches are now possible

#111787 - $15.00 USD Received 22 May 2009; revised 26 Jun 2009; accepted 28 Jun 2009; published 13 Jul 2009

to reconstruct the light field diffracted by the object. In the first approach, three interferograms with the same size of the original one, $I(x,y,0)$, $I(x,y,\pi/2)$, and $I(x,y,\pi)$ are generated by extracting the values of the original interferogram periodically at locations with the same phase shift, and using linear interpolation to allocate the empty pixels. Interpolation is performed by averaging the values of adjacent pixels in a similar way as is done in Refs [24–26]. Note that the interpolation is more accurate for the interferogram with a $\pi/2$ shift, as we have information in two pixels of the unit cell.

In this way, it can be shown that, the complex field generated by the object beam at the output plane, our digital hologram, can be written as

$$O(x,y,0)=\frac{1}{4}\left\{I(x,y,0)-I(x,y,\pi)+i\left[2I(x,y,\pi/2)-I(x,y,0)-I(x,y,\pi)\right]\right\}. \quad (7)$$

This equation is directly obtained by expanding each interferogram in terms of the real and imaginary parts of the complex amplitude distribution associated to both the object and the reference patterns at the output plane and assuming a parallel reference beam.

In the second approach, Eq. (7) is used to interpolate a single discrete value of the digital hologram O for each unit cell of the original interferogram. In this case, the final hologram is half the size of the previous one in each transversal dimension. We choose to use the first approach since it has been shown in other interferometry applications that it gives slightly better results than the second one [23].

The resulting complex digital hologram, $O(x,y,0)$ allows us to reconstruct numerically the complex amplitude distribution, $O(x,y,z)$, generated by the 3D object at plane located at a distance z from the sensor. The reconstruction can be obtained by computing a discrete Fresnel integral or, alternatively, by using the propagation transfer function method, i.e.,

$$O(m,n;z)=F^{-1}\left\{F\left[O(m,n,0)\right]\exp\left[-i\pi\lambda z\left(\frac{u^2}{(\Delta x N_x)^2}+\frac{v^2}{(\Delta y N_y)^2}\right)\right]\right\}, \quad (8)$$

where F denotes the fast Fourier transform, (u,v) are discrete spatial frequency variables, (m,n) are discrete transversal spatial coordinates in both the CCD plane and the output plane, and N_x and N_y are the number of samples in the x and y directions. Note that negative values of z are to be considered to simulate backward propagation in Eq. (8). In this approach, the resolution at the output plane is the same for any propagation distance z, and is given by the resolution at the input plane, i.e., the size of the pixel $(\Delta x,\Delta y)$ in the CCD sensor.

3. Numerical simulations

We performed numerical simulations of the Talbot digital holography system depicted in Fig. 1 to validate our proposal. We assumed a parallel light beam with wavelength λ = 514.5 nm illuminating two 2D objects located at different distances from the CCD, z_1 = 400 mm for the case of the object shown in Fig. 3(a) and z_2 = 300 mm for the one in Fig. 3(b). A random phase mask was attached to the binary images to spread the diffraction patterns at the output plane. The CCD sensor is supposed to have $N_x \times N_y$ = 1024 × 1024 pixels with size $\Delta x = \Delta y$ = 9 μm. Following our reasoning in the previous section we simulate a binary amplitude grating (see Fig. 2) with an open ratio equal to 0.5 and a period d = 18 μm, double of the pixel size, in both dimensions located in the reference beam of the interferometer. By application of Eq. (3) we calculate the Talbot distance z_t = 1.26 mm and the distance from the grating to the CCD to obtain the Fresnel image with q = 1 and n/m = 3/4, i.e., z' = 2.20 mm.

The diffraction pattern generated by both 2D objects at the output plane was evaluated by using the propagation transfer function method, and so was done to evaluate the Fresnel image generated by the grating. From the interference between these fields we generated three interpolated interferograms for each phase shift. The digital hologram was then evaluated by using Eq. (7) and, finally, we used Eq. (8) to reconstruct the objects at distances z_1 and z_2.

#111787 - $15.00 USD Received 22 May 2009; revised 26 Jun 2009; accepted 28 Jun 2009; published 13 Jul 2009

(a) (b)

Fig. 3. Pictures of the irradiance distribution associated to the input 2D objects located at the object beam of the optical system depicted in Fig. 3. Objects (a) and (b) are assumed to be at a distance z_1 = 400mm and z_2 = 300 mm from the CCD sensor, respectively.

The results are shown in Fig. 4. Figure 4(a) shows the irradiance distribution associated to the interferogram at the output plane of the Talbot digital holography system in Fig. 1 obtained by the interference between the Fresnel diffraction patterns of both 2D objects in Fig. 3 and the Fresnel image of the grating. Figures 4 (b) and (c) are reconstructed images of the objects obtained by computing the inverse Fresnel diffraction pattern from the corresponding digital hologram. Note that the objects are clearly reconstructed. Small artifacts in these pictures are due basically to the random phase mask attached to the objects but also because of the interpolation procedure.

4. Experimental results

The Talbot digital holographic system in Fig. 1 was assembled in the laboratory to record the digital holograms of several 2D objects located at different distances. The light source is an Ar laser operating at 514.5 nm. The sensor is a monochrome CCD camera with 2024 × 2024 pixels with size equal to $9 \times 9\ \mu m^2$.

(a) (b) (c)

Fig. 4. Gray level pictures corresponding to the results of the numerical simulation: (a) Talbot interferogram at the output plane of the optical system in Fig. 1, (b) and (c) reconstructed images at two different distances from the resulting digital hologram. The Fresnel image projected onto the sensor plane corresponds to that obtained at a distance from the grating given by $(1 + 3/4)z_t$.

The amplitude mask at the reference beam is a 2D binary square grating with size 2 × 2 cm^2, period d = 144 μm and opening ratio 0.5, manufactured in our laboratory by laser photolithography on a chrome photomask. The photomask was a quartz substrate (size 2 × 2 × 0.09 inch) coated with a low reflectivity chromium layer (thickness 120 nm) and S1805 photoresist film (*Shipley*). The blank was irradiated by using a laser writing machine (*Microtech, srl*). The final mask was obtained by developing the photoresist with MF319 developer (*Shipley*), etching the unprotected chromium, and cleaning the remaining photoresist. The Talbot distance for this grating is z_t = 80.6 mm. Figure 5(a) shows a central region of the irradiance distribution of the first self-image of the grating recorded by the CCD.

#111787 - $15.00 USD Received 22 May 2009; revised 26 Jun 2009; accepted 28 Jun 2009; published 13 Jul 2009

The distance from the grating to the CCD was then adjusted to obtain a Fresnel image with q = 1 and n/m = 3/4. Figure 5(b) shows the irradiance distribution (approximately uniform) generated by the Fresnel image on the CCD while Fig. 5(c) is a gray level picture of the interference pattern generated when a parallel light beam is used as object beam in the interferometer. Note the periodic three-step phase distribution (with values 0, $\pi/2$ and π) associated to the Fresnel image. The requirements established in Eq. (6) to get high quality Fresnel images are fulfilled by using a parallel light beam with 15 mm diameter as. In this way, we illuminate around 100 periods of the grating.

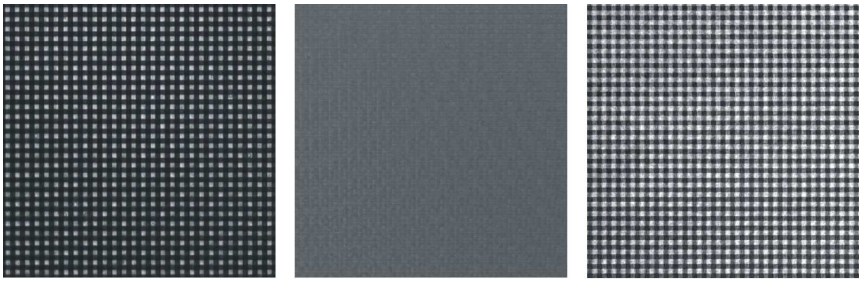

(a) (b) (c)

Fig. 5. Gray level pictures of a central region of the light distribution generated by the grating at the output plane of the system in Fig. 1: (a) Irradiance distribution of the first self image, (b) uniform irradiance distribution of the Fresnel image with $z' = (1 + 3/4)z_t$, (c) interference pattern between the same Fresnel image and a parallel object beam showing the periodic three-step phase distribution.

The objects positioned in the object beam were 2D transparencies with an approximate size of 1.3 × 1.3 cm^2 located at different distances. The first transparency codifies the binary object shown in Fig. 3(a) and was located at a distance of 32 cm from the CCD. The second corresponds to the object in Fig. 3(b), at a distance of 37 cm, while the third object was a USAF resolution target located at 42 cm from the sensor.

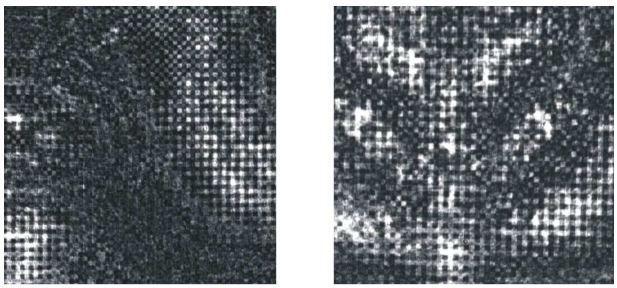

(a) (b)

Fig. 6. Gray-level pictures of a partial region of the interference patterns generated at the output plane of the Talbot holography system in Fig. 1 for different 2D objects located at the object beam: (a) the object in Fig. 3(a) and (b) the object in Fig. 3(b). The grating located at the reference beam generates the Fresnel image corresponding to $z' = (1 + 3/4)z_t$. Note the pixelated structure.

The interferogram between the object diffraction patterns and the Talbot codified reference beam was recorded with a single shot of the CCD. Figure 6 shows a central region of the result for the first two objects. It is possible to note the pixelated structure of the recorded interferogram because of the periodic structure of the Fresnel image. The digital hologram is then obtained by interpolation and applying Eq. (7). In our preliminary experiment, the period of the grating was chosen as large as 16 times the sensor pixel size to get an adequate value of the Talbot distance to locate the different optical elements in Fig. 1 without difficulty, but also to improve the tolerance to transversal misalignments. In this way,

#111787 - $15.00 USD Received 22 May 2009; revised 26 Jun 2009; accepted 28 Jun 2009; published 13 Jul 2009

each square of constant phase in Fig. 6 has a size of 72 × 72 μm^2, corresponding to 8 × 8 pixels of the camera, and the resolution of our final hologram (with only 256 × 256 complex values) is 8 times lower than the maximum achievable.

Once the digital holograms were recorded, images of the objects were reconstructed evaluating the Fresnel diffraction integral in the computer by using a fast Fourier transform algorithm. The results are shown in pictures (a), (b), and (c) in Fig. 7. These results confirm the feasibility and flexibility of our method.

(a) (b) (c)

Fig. 7. Gray level pictures showing the result of the reconstruction of the different digital holograms recorded experimentally: (a), (b), and (c) show the reconstruction of the objects in Fig. 3(a), Fig. 3(b) and the USAF resolution target, respectively.

5 Conclusions

We have proposed a dynamic digital holography system based on a three-step phase shifting technique obtained by the fractional Talbot effect. The basic idea consists in using a 2D binary grating codifying the reference beam of a conventional Match-Zehnder interferometer. In this way, a periodic three-step phase distribution with uniform irradiance is generated by the reference beam over the sensor plane by fractional Talbot effect. The interference of this diffraction pattern with the light diffracted by an object allows measuring the Fresnel digital hologram of the object with one single shot of the light sensor. The light field diffracted by the object at different distances can then be reconstructed from the digital hologram.

The proposed Talbot digital holography system has some limitations common to most dynamic or parallel holographic methods based on spatial division-multiplexing. As in previous proposals, the increase in time resolution is at the expense of a decrease in spatial resolution. However this is unavoidable to develop dynamic applications of digital holography. Also, as we use binary amplitude gratings, a fraction of light is lost by absorption in the mask. Nevertheless, as the grating is in the reference beam, this missing energy can be easily compensated.

Conversely, our proposal has several advantages over previous systems. The optical setup is simple and compact, as in off-axis geometries, but it does not require using a tilted reference beam and allows one to suppress the zero order and the defocused twin image term efficiently with phase-shifting techniques. In contrast with other phase-shifting techniques we do not need special phase diffractive elements to make several copies of the object and reference beams. Neither we need complex pixelated polarization devices, which are difficult to build and hard to integrate with the CCD sensor. Our codifying mask is very simple and commercially available, as two conventional square 1D gratings can be combined in orthogonal directions to codify the reference beam. Alternatively, it can be easily fabricated by standard lithographic techniques as we did in our laboratory. Furthermore, because of the amplitude modulation, the mask is not sensitive to the wavelength. Therefore, under parallel illumination, we only need to shift axially the grating to obtain the same Fresnel image, and with the same scale, for different wavelengths. Moreover, Fresnel images are generated by free-space propagation avoiding the use of lenses that can introduce aberrations.

#111787 - $15.00 USD Received 22 May 2009; revised 26 Jun 2009; accepted 28 Jun 2009; published 13 Jul 2009

Simulations and experiments were performed with 2D objects but their extension to 3D scenes and/or microscopy is obvious and will be the subject of future work. Also, the results can be further improved by using codifying gratings with a smaller period and well adapted to the sensor pixel size. However, computer simulations and preliminary experimental results confirm the feasibility and flexibility of our method.

Acknowledgments

The authors are very grateful to the *Serveis Centrals d' Intrumentació Científica (SCIC)* of the *Universitat Jaume I* for the use of the lithography system based on direct laser writing. This work has been supported in part by the agreement between the *Universitat Jaume I* and the *Fundació Caixa Castelló (Bancaixa)*, grant P1-1B2006-29. Maria A. Araiza-E gratefully acknowledges a grant, 08I011.36/1, from the same agreement and partial support by PROMEP PIFI 2007-33-07, México. B. Javidi is grateful for support from Guggenheim Foundation.

#111787 - $15.00 USD Received 22 May 2009; revised 26 Jun 2009; accepted 28 Jun 2009; published 13 Jul 2009